RLS ALGORITHM FOR A NEW SUBBAND ADAPTIVE STRUCTURE WITH CRITICAL SAMPLING

R. G. Alves[1,2], *M.R. Petraglia*[1], *J. A. Apolinário Jr.*[1,3], *and P. S. R. Diniz*[1]

[1]Federal University of Rio de Janeiro
COPPE - Program of Electrical Engineering
CP 68564, CEP 21945-970
Rio de Janeiro, RJ - Brazil
[2]National Institute of Metrology
DIMCI/DIELE/LATCE
CP 94501, CEP 25250-020
Duque de Caxias, RJ - Brazil
[3]Military Institute of Engineering
Department of Electrical Engineering
Praça Gen Tibúrcio, 80
Rio de Janeiro, RJ - Brazil
e-mails: guedes@lps.ufrj.br, mariane@coe.ufrj.br, apolin@epq.ime.eb.br, and diniz@lps.ufrj.br

Abstract – In a recent publication a new family of adaptive structures with critical sampling of the subband signals, which yields exact modeling of FIR systems, was obtained. In this paper an algorithm based on the recursive least-squares (RLS) algorithm is derived for the updating of the adaptive coefficients of this new subband structure. An efficient implementation of the resulting structure is discussed, leading to computational complexity savings. Computer simulations ilustrate the convergence behavior of the proposed algorithm.

I. INTRODUCTION

Adaptive FIR filters are attractive in many applications due to their stability and unimodal performance surface properties. However, when the order of such filters is very high, a large number of operations is needed for their implementation and the adaptation algorithm presents slow convergence. Alternative structures that make use of multirate concepts have been proposed [1]-[3] with the objective of reducing the drawbacks described above. In most of these subband structures, the signals at the outputs of the analysis filter bank are down-sampled and the adaptation is performed at the reduced sampling rate, which leads to large computational savings for high-order filters, with the introduction of an extra input-output delay. In order to model a finite impulse response system with small asymptotic errors, the adaptive subband structure with critical sampling requires additional adaptive cross-terms among the subbands [1]. These cross-terms, however, increase the computational complexity and reduce the convergence rate of the adaptive algorithm. In [3] a new family of adaptive structures with critical sampling of the subband signals, which also yields exact modeling of FIR systems, was obtained. The resulting structures also present extra filters among the subbands, but such filters are related to the direct-path adaptive filters, and do not need to be adapted separately. Therefore, the computational complexity is reduced and the adaptation speed is improved when compared to the algorithms derived in [1]. In this paper, an adaptation algorithm based on the RLS algorithm is derived for the updating of the subfilter coefficients. The convergence behavior of the proposed adaptive subband algorithm is illustrated by computer simulations and compared to the behavior of the full-band RLS algorithm.

II. THE NEW ADAPTIVE SUBBAND STRUCTURE WITH CRITICAL SAMPLING

The new family of adaptive subband structures was derived from the filter bank structure with adaptive sparse subfilters of Fig. 1(a), which can be redrawn as in Fig. 1(b) by making use of the polyphase matrix of the analysis filter bank $\boldsymbol{H}_p(z)$. In a system identification application, the coefficients of the adaptive filter structure are updated in order to model an unknown FIR system, denoted here by $P(z)$. The polyphase representation

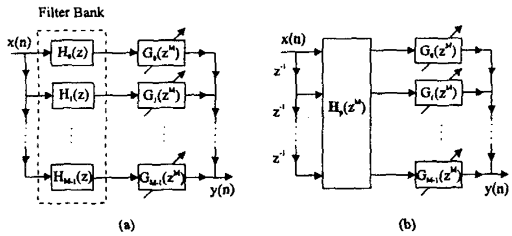

Figure 1: Adaptive structure: (a) with an analysis filter bank and sparse subfilters; (b) with polyphase representation of the analysis filter bank.

of $P(z)$ is shown in Fig. 2(a). Including before the polyphase components $P_k(z)$ in Fig. 2(a) the matrices $\boldsymbol{H}_p(z^M)$ and $\boldsymbol{F}_p(z^M)$, as shown in Fig. 2(b), such that $\boldsymbol{F}_p(z)\boldsymbol{H}_p(z) = z^{-\Delta}\boldsymbol{I}_M$, where $\boldsymbol{I}_M$ is the $M \times M$ identity matrix, the transfer function of the system is not altered. The matrices $\boldsymbol{H}_p(z)$ and $\boldsymbol{F}_p(z)$ that satisfy the above condition correspond to the polyphase matrices of the analysis and synthesis filter banks, respectively, of a perfect reconstruction multirate system. Figures 1(b) and 2(b)

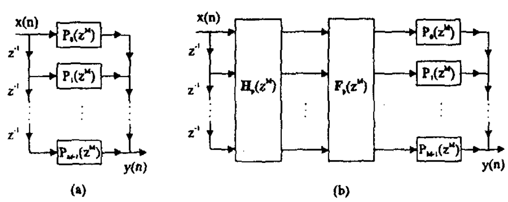

Figure 2: Unknown system: (a) polyphase decomposition; (b) equivalent representation with perfect reconstruction polyphase matrices.

are equivalent, that is, both structures implement the transfer function $z^{-M\Delta}P(z)$ when

$$\begin{bmatrix} G_0(z) & G_1(z) & \cdots & G_{M-1}(z) \end{bmatrix} = \begin{bmatrix} P_0(z) & P_1(z) & \cdots & P_{M-1}(z) \end{bmatrix} \boldsymbol{F}_p(z). \quad (1)$$

Therefore, by using an analysis filter bank which yields perfect reconstruction and adaptive subfilters of sufficient order such that Eq. (1) can be satisfied, the structure of Fig. 1(a) can implement exactly any FIR system. Now, including maximally decimated perfect reconstruction analysis and synthesis banks following each sparse subfilter in Fig. 1(a), moving the sparse subfilters $G_k(z^M)$ to the right of the decimators (becoming $G_k(z)$ by the *noble identity* [4]), and assuming that non-adjacent filters of the analysis bank have frequency responses which do not overlap, the structure of Fig. 3 is obtained. Observe that in the resulting structure only M subfilters need to be adapted, namely $G_0(z), \cdots, G_{M-1}(z)$, and that they operate at a rate which is $1/M$-th of the input rate. From Eq. (1), the length of each subfilter $G_k(z)$ must be $K = (N_p + N_f)/M$, where N_p is the length of the system $P(z)$ to be identified and N_f is the length of the synthesis filter $F_k(z)$, which is equal to the length (N_h) of the analysis filter $H_k(z)$.

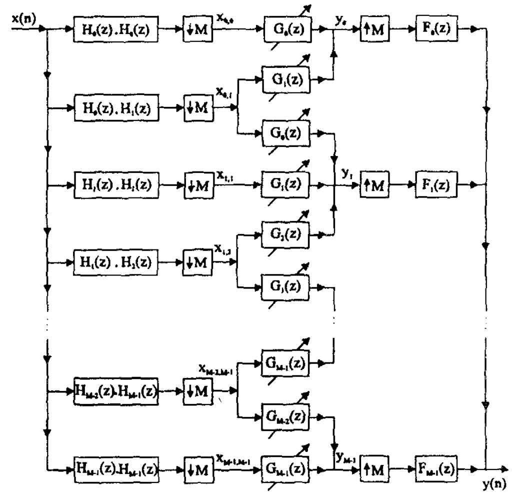

Figure 3: New adaptive subband structure.

III. ADAPTATION ALGORITHM IN SUBBAND BASED ON THE RLS ALGORITHM

The extension of the RLS fullband algorithm [6] for an M-subband system leads to the minimization of the following objective function:

$$J(k) = \sum_{i=0}^{M-1} \sum_{j=0}^{k} \lambda_i^{k-j} e_i^2(j) \quad (2)$$

where M is the number of subbands of the system, k is the time index, λ_i is the forgetting factor of the i-th subband and e_i is the error signal of the i-th subband that is described according to the following equation:

$$\begin{aligned} e_i(k) &= d_i(k) - [\boldsymbol{x}_{i-1,i}^T(k)\boldsymbol{G}_{i-1}(k) + \boldsymbol{x}_{i,i}^T(k)\boldsymbol{G}_i(k) \\ &+ \boldsymbol{x}_{i,i+1}^T(k)\boldsymbol{G}_{i+1}(k)] \end{aligned} \quad (3)$$

where $\boldsymbol{x}_{i,j}(k) = [x_{i,j}(k)\ x_{i,j}(k-1)\ \cdots\ x_{i,j}(k-K-1)]^T$, $x_{i,j}$ are the signals after the down-samplers as can be seen in Fig. 3, $d_i(k)$ is the reference signal for subband i, and the column vectors $\boldsymbol{G}_i(k)$ have dimension $K \times 1$ and contain the coefficients of the adaptive subfilters. It is worth mentioning that in the expression of the subband error in the above equation, we have assumed that only adjacent subbands have overlap.

By substituting Eq. (3) in Eq. (2) and considering $\lambda_i = \lambda$ for $i = 0, 1, ..., M-1$ in order to simplify the notation, we can rewrite Eq. (2) as:

$$\begin{aligned} J(k) &= \sum_{i=0}^{M-1} [\boldsymbol{d}_i(k) - \boldsymbol{X}^T_{i-1,i}(k)\boldsymbol{G}_{i-1}(k) \\ &- \boldsymbol{X}^T_{i,i}(k)\boldsymbol{G}_i(k) \\ &- \boldsymbol{X}^T_{i,i+1}(k)\boldsymbol{G}_{i+1}(k)]^T[\boldsymbol{d}_i(k) \\ &- \boldsymbol{X}^T_{i-1,i}(k)\boldsymbol{G}_{i-1}(k) \\ &- \boldsymbol{X}^T_{i,i}(k)\boldsymbol{G}_i(k) - \boldsymbol{X}^T_{i,i+1}(k)\boldsymbol{G}_{i+1}(k)] \end{aligned} \quad (4)$$

where

$$\boldsymbol{d}_i(k) = \begin{bmatrix} d_i(k) \\ \lambda^{1/2} d_i(k-1) \\ \vdots \\ \lambda^{k/2} d_i(0) \end{bmatrix} \quad (5)$$

for $i = 0, 1, \cdots, M-1$, and

$$\begin{aligned} \boldsymbol{X}_{i,j}(k) &= \\ &\begin{bmatrix} x_{i,j}(k) & \cdots & \lambda^{(k-1)/2}x_{i,j}(1) & \lambda^{k/2}x_{i,j}(0) \\ x_{i,j}(k-1) & \cdots & \lambda^{(k-1)/2}x_{i,j}(0) & 0 \\ \vdots & \cdots & \vdots & \vdots \\ x_{i,j}(k-K-1) & \cdots & 0 & 0 \end{bmatrix} \\ &= \begin{bmatrix} \boldsymbol{x}_{i,j}(k) & \lambda^{1/2}\boldsymbol{x}_{i,j}(k-1) & \cdots & \lambda^{k/2}\boldsymbol{x}_{i,j}(0) \end{bmatrix} \end{aligned} \quad (6)$$

for $i = 0, 1, \cdots, M-1$ and $j = i, i+1$.

In Eq. (4) (and hereafter) it was assumed that $\boldsymbol{X}_{-1,0}(k) = \boldsymbol{0}$, $\boldsymbol{G}_{-1}(k) = \boldsymbol{0}$, $\boldsymbol{X}_{M-1,M}(k) = \boldsymbol{0}$, and $\boldsymbol{G}_M(k) = \boldsymbol{0}$ for the first and the last subbands ($i = 0$ and $i = M-1$). Note that $\boldsymbol{d}_i(k)$ is $(k+1) \times 1$ and that matrix $\boldsymbol{X}_{i,j}(k)$ is $K \times (k+1)$.

In order to clarify the variables described above, Fig. 4 depicts the whole two-subband system including the filter banks, the adaptive structure, and the generation of the reference signal ($d(k)$) in a system identification setup. Note that $N(k)$ is the observation noise and that Δ — which is given by $(N_h + N_f)/2M$) — is necessary to generate the error signals due to different delays of y_i and d_i caused by this subband structure.

From Eq. (4), we calculate the partial derivatives of $J(k)$ with respect to $\boldsymbol{G}_i(k)$ and by making them

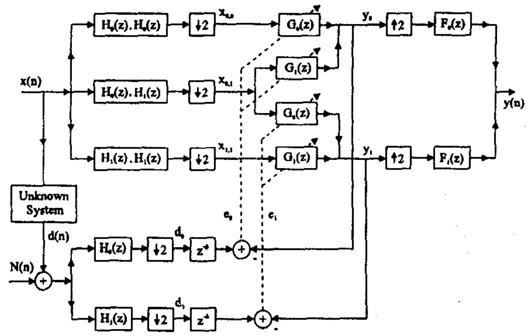

Figure 4: Example of a two-subband system applied in a system identification problem.

equal to zero, we minimize the objective function and obtain the following result:

$$\begin{bmatrix} \boldsymbol{A}_0(k) & \boldsymbol{B}_0(k) & \boldsymbol{C}_0(k) & \boldsymbol{0} & \cdots & \cdots & \boldsymbol{0} \\ \boldsymbol{B}_0^T(k) & \boldsymbol{A}_1(k) & \boldsymbol{B}_1(k) & \boldsymbol{C}_1(k) & \ddots & \cdots & \vdots \\ \boldsymbol{C}_0^T(k) & \boldsymbol{B}_1^T(k) & \boldsymbol{A}_2(k) & \boldsymbol{B}_2(k) & \boldsymbol{C}_2(k) & \ddots & \vdots \\ \boldsymbol{0} & \ddots & \ddots & \ddots & \ddots & \ddots & \boldsymbol{0} \\ \vdots & \vdots & \ddots & \ddots & \ddots & \ddots & \boldsymbol{C}_{M-3}(k) \\ \vdots & \vdots & \vdots & \ddots & \ddots & \ddots & \boldsymbol{B}_{M-2}(k) \\ \boldsymbol{0} & \cdots & \cdots & \boldsymbol{0} & \boldsymbol{C}^T_{M-3}(k) & \boldsymbol{B}^T_{M-2}(k) & \boldsymbol{A}_{M-1}(k) \end{bmatrix} \cdot \begin{bmatrix} \boldsymbol{G}_0(k) \\ \boldsymbol{G}_1(k) \\ \boldsymbol{G}_2(k) \\ \vdots \\ \vdots \\ \boldsymbol{G}_{M-1}(k) \end{bmatrix} = \begin{bmatrix} \boldsymbol{p}_0(k) \\ \boldsymbol{p}_1(k) \\ \boldsymbol{p}_2(k) \\ \vdots \\ \vdots \\ \boldsymbol{p}_{M-1}(k) \end{bmatrix} \quad (7)$$

where

$$\begin{aligned} \boldsymbol{A}_i(k) &= \boldsymbol{X}_{i,i}(k)\boldsymbol{X}^T_{i,i}(k) + \boldsymbol{X}_{i-1,i}(k)\boldsymbol{X}^T_{i-1,i}(k) \\ &+ \boldsymbol{X}_{i,i+1}(k)\boldsymbol{X}^T_{i,i+1}(k) \quad (8) \\ \boldsymbol{B}_i(k) &= \boldsymbol{X}_{i,i}(k)\boldsymbol{X}^T_{i,i+1}(k) + \boldsymbol{X}_{i,i+1}(k)\boldsymbol{X}^T_{i+1,i+1}(k) \quad (9) \\ \boldsymbol{C}_i(k) &= \boldsymbol{X}_{i,i+1}(k)\boldsymbol{X}^T_{i+1,i+2}(k) \quad (10) \\ \boldsymbol{p}_i(k) &= \boldsymbol{X}_{i-1,i}(k)\boldsymbol{d}_{i-1}(k) + \boldsymbol{X}_{i,i}(k)\boldsymbol{d}_i(k) \\ &+ \boldsymbol{X}_{i,i+1}(k)\boldsymbol{d}_{i+1}(k) \quad (11) \end{aligned}$$

Expressing Eq. (7) in the form

$$\boldsymbol{R}_{D,M}(k)\boldsymbol{G}(k) = \boldsymbol{p}_{D,M}(k) \quad (12)$$

we observe that the matrix $\boldsymbol{R}_{D,M}(k)$ (D and M in this case stand for *deterministic* and the *M number of subbands*), that we need to invert in order to get the optimal solution, has a recursive form as in the fullband RLS algorithm and can be written as

$$\boldsymbol{R}_{D,M}(k) = \lambda \boldsymbol{R}_{D,M}(k-1) + \boldsymbol{\mathcal{X}}(k)\boldsymbol{\mathcal{X}}^T(k) \quad (13)$$

where

$$\boldsymbol{\mathcal{X}}(k) = \begin{bmatrix} x_{0,0}(k) & x_{0,1}(k) & 0 & \cdots & 0 \\ x_{0,1}(k) & x_{1,1}(k) & x_{1,2}(k) & \ddots & \vdots \\ 0 & \ddots & \ddots & \ddots & 0 \\ \vdots & \ddots & \ddots & \ddots & x_{M-2,M-1}(k) \\ 0 & \cdots & 0 & x_{M-2,M-1}(k) & x_{M-1,M-1}(k) \end{bmatrix} \quad (14)$$

By observing Eq. (13), we verify that we can apply the so-called *matrix inversion lemma* given by [6]

$$[\mathcal{A}+\mathcal{B}\mathcal{C}\mathcal{D}]^{-1} = \mathcal{A}^{-1}-\mathcal{A}^{-1}\mathcal{B}[\mathcal{D}\mathcal{A}^{-1}\mathcal{B}+\mathcal{C}^{-1}]^{-1}\mathcal{D}\mathcal{A}^{-1} \quad (15)$$

for the subband RLS algorithm in the same way as it is used in the RLS fullband case by making $\mathcal{A} = \lambda \boldsymbol{R}_{D,M}(k-1)$, $\mathcal{B} = \boldsymbol{\mathcal{X}}(k)$, $\mathcal{C} = \boldsymbol{I}_M$, and $\mathcal{D} = \boldsymbol{\mathcal{X}}^T(k)$. The resulting expression is given by

$$\begin{aligned} \boldsymbol{S}_{D,M}(k) = \boldsymbol{R}_{D,M}^{-1}(k) = \frac{1}{\lambda}\{\boldsymbol{S}_{D,M}(k-1) \\ -\boldsymbol{S}_{D,M}(k-1)\boldsymbol{\mathcal{X}}(k)[\lambda \boldsymbol{I}_M \\ +\boldsymbol{\mathcal{X}}^T(k)\boldsymbol{S}_{D,M}(k-1)\boldsymbol{\mathcal{X}}(k)]^{-1} \\ .\boldsymbol{\mathcal{X}}^T(k)\boldsymbol{S}_{D,M}(k-1)\} \end{aligned} \quad (16)$$

In the last equation, the matrices $\boldsymbol{S}_{D,M}(k-1)$ and $\boldsymbol{\mathcal{X}}(k)$ have dimensions $MK \times MK$ and $MK \times M$, respectively. It is worth mentioning that the expression $[\mathcal{D}\mathcal{A}^{-1}\mathcal{B}+\mathcal{C}^{-1}]^{-1}$ is an $M \times M$ matrix whose inverse can be easily calculated.

The following equations, together with Eq. (16), define the subband RLS algorithm:

$$\begin{aligned} \boldsymbol{p}_{D,M}(k) &= \lambda \boldsymbol{p}_{D,M}(k-1) + \boldsymbol{\mathcal{X}}(k)\boldsymbol{d}(k) & (17) \\ \boldsymbol{G}(k) &= \boldsymbol{S}_{D,M}(k)\boldsymbol{p}_{D,M}(k) & (18) \\ \boldsymbol{y}(k) &= \boldsymbol{\mathcal{X}}^T(k)\boldsymbol{G}(k) & (19) \\ \boldsymbol{e}(k) &= \boldsymbol{d}(k) - \boldsymbol{y}(k) & (20) \end{aligned}$$

where $\boldsymbol{d}(k)$, $\boldsymbol{y}(k)$, and $\boldsymbol{e}(k)$ are given by $[d_0(k) \quad d_1(k) \quad \cdots d_{M-1}(k)]^T$, $[y_0(k) \quad y_1(k) \quad \cdots \quad y_{M-1}(k)]^T$, and $[e_0(k)\ e_1(k) \cdots e_{M-1}(k)]^T$, respectively.

Observe that we have obtained a solution for the new subband structure similar to that of the fullband structure. Moreover a recursive form for $\boldsymbol{S}_{D,M}(k)$ has also being obtained as in the fullband RLS algorithm. Therefore, subband RLS algorithm is very similar to the conventional RLS algorithm and is presented in Table I.

TABLE I
THE SUBBAND RLS ALGORITHM.

Initialization:
$\boldsymbol{S}_{D,M} = \delta \boldsymbol{I}_{MK}$
where δ can be the inverse of the input-signal power estimate
$\boldsymbol{p}_{D,M}(k) = [0 \ 0 \ \cdots \ 0]^T$
For $k \geq 0$:
$\boldsymbol{S}_{D,M}(k) = \frac{1}{\lambda}\{\boldsymbol{S}_{D,M}(k-1)-$
$\boldsymbol{S}_{D,M}(k-1)\boldsymbol{\mathcal{X}}(k)\,[\lambda \boldsymbol{I}_M$
$+\boldsymbol{\mathcal{X}}^T(k)\boldsymbol{S}_{D,M}(k-1)\boldsymbol{\mathcal{X}}(k)\big]^{-1}$
$\boldsymbol{\mathcal{X}}^T(k)\boldsymbol{S}_{D,M}(k-1)\}$
$\boldsymbol{p}_{D,M}(k) = \lambda \boldsymbol{p}_{D,M}(k-1) + \boldsymbol{\mathcal{X}}(k)\boldsymbol{d}(k)$
$\boldsymbol{G}(k) = \boldsymbol{S}_{D,M}(k)\boldsymbol{p}_{D,M}(k)$
If necessary compute the output and the error
$\boldsymbol{y}(k) = \boldsymbol{\mathcal{X}}^T(k)\boldsymbol{G}(k)$
$\boldsymbol{e}(k) = \boldsymbol{d}(k) - \boldsymbol{y}(k)$

IV. COMPUTATIONAL COMPLEXITY

In this section we compare the computational complexity of the conventional and the subband RLS using as criterion the number of multiplications necessary for computing the inverse of $\boldsymbol{R}_{D,M}(k)$, since the computational burden for calculating the other terms is approximately the same.

- Fullband RLS Complexity

  Considering the implementation of the conventional RLS algorithm, the number of multiplications for inverting the matrix $\boldsymbol{R}_D(k)$ using the *matrix inversion lemma* is equal to:

$$2N_p^2 + N_p \quad (21)$$

- Subband RLS Complexity

  In the computation of the inverse of $\boldsymbol{R}_{D,M}(k)$ we use Eq. (16), and for better explanation of the computational complexity we divide the expression in two parts:

  - Computational complexity for calculating $\mathcal{Z} = [\lambda \boldsymbol{I}_M + \boldsymbol{\mathcal{X}}^T(k)\boldsymbol{S}_{D,M}(k-1)\boldsymbol{\mathcal{X}}(k)]^{-1}$: since $\boldsymbol{S}_{D,M}(k-1)$ is an $(MK \times MK)$ matrix and $\boldsymbol{\mathcal{X}}^T(k)$ is an $(M \times MK)$ matrix with only $3K$ non-null elements in each row, the product $\boldsymbol{\mathcal{X}}^T(k)\boldsymbol{S}_{D,M}(k)$ will require $3M^2K^2$ multiplications. The resulting matrix will have dimension $(M \times MK)$ and will be post-multiplied by $\boldsymbol{\mathcal{X}}(k)$ which has dimension $(MK \times M)$, requiring $3M^2K$ multiplications.

The resulting matrix (after adding $\lambda \boldsymbol{I}_M$) will have dimension $(M \times M)$ and for computing its inverse approximately M^3 multiplications will be necessary (actually the computational complexity for calculating the inverse of a matrix using Givens triangularization is $2/3M^3$ multiplications plus M squared roots plus the cost of the backsubstitution procedure). The total number of multiplications for this part of Eq. (16) is then $(3M^2K^2 + 3M^2K + M^3)$.

- Computational complexity for calculating $\boldsymbol{S}_{D,M}(k-1)\boldsymbol{\mathcal{X}}(k)\boldsymbol{Z}\boldsymbol{\mathcal{X}}^T(k)\boldsymbol{S}_{D,M}(k-1)$: the product $\boldsymbol{\mathcal{X}}^T(k)\boldsymbol{S}_{D,M}(k-1)$ was discussed above, and the product $\boldsymbol{S}_{D,M}(k-1)\boldsymbol{\mathcal{X}}(k)$ is equal to the transpose of $\boldsymbol{\mathcal{X}}^T(k)\boldsymbol{S}_{D,M}(k-1)$. Then, in this part of the expression in Eq. (16), we have to compute the computational complexity of the multiplication of three matrices with dimensions $(MK \times M)$, $(M \times M)$, and $(M \times MK)$, that will lead us to the amount of $M^3K + M^3K^2$ multiplications. We are not considering here the savings due to the symmetry of the resulting matrix since this consideration was not taken into account in the computational complexity of the fullband RLS algorithm.

Therefore the total computational complexity for calculating $S_{D,M}(k)$ is:

$$\frac{3M^2K^2 + M^3K^2 + M^3K + 3M^2K + M^3}{M} \qquad (22)$$

The division by M is because the update of the coefficients in the subband is done in a rate M times lower than the rate used in the fullband algorithm.

If we substitute in Eq. (22) the length K of the adaptive subfilter by $((N_p + N_f)/M)$, we obtain

$$\frac{(3+M)(N_p+N_f)^2 + (M^2+3M)(N_p+N_f) + M^3}{M} \qquad (23)$$

where we observe that the number of multiplications obtained in the fullband RLS algorithm is approximately $2M/(M+3)$ times higher than that of the subband RLS algorithm for small N_f. Observe however that the number of coefficients of $F_i(z)$ is related to the desired level of mean-square error (MSE).

It is worth mentioning that the computational complexity for the implementation of the filter bank of the proposed structure using the cosine modulated method is $\frac{2(3N_h-2)}{M} + 4log_2M$ [3] which is considerably smaller than the result obtained in Eq. (23).

V. SIMULATION RESULTS

The identification of a length $N_p = 256$ FIR system is considered. The input signal is either a white noise sequence of unit variance or a colored noise sequence generated by filtering a white noise sequence by a first-order IIR filter with a single pole located at $z = 0.9$. Experiments were carried out with the subband structure of Fig. 3 for $M = 4$ subbands and using perfect reconstruction analysis and synthesis cosine modulated filter banks with prototype filter of length $N_h = 48$ [4]. The length of the subfilters was $K = 76$ and the forgetting factor was $\lambda = 0.95$ for both fullband and subband RLS algorithms. Moreover, the variance of the observation noise is 10^{-10}.

Figure 5 depicts the MSE evolution with white-noise input signal. We can see that the proposed subband algorithm presents a convergence rate that, although similar to that of the fullband RLS algorithm, has a delay due to the structure. The proposed structure converges to an MSE of the order of the stopband attenuation of the analysis filter (which is around −60 dB), due to the unrealistic assumption of non-overlapping of non-adjacent analysis filters.

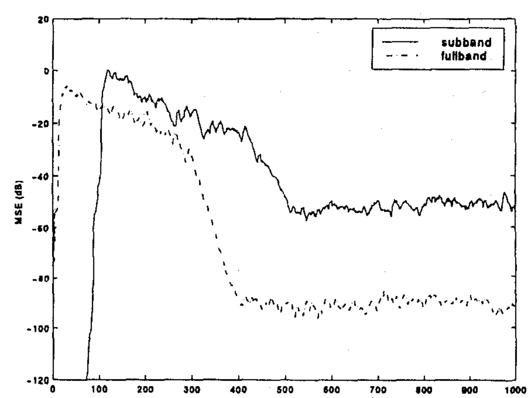

Figure 5: Simulation results with white-noise input.

Figure 6 presents the MSE evolution of the algorithms with colored input signal. This figure shows that the convergence rate is practically the same as for white noise input as expected.

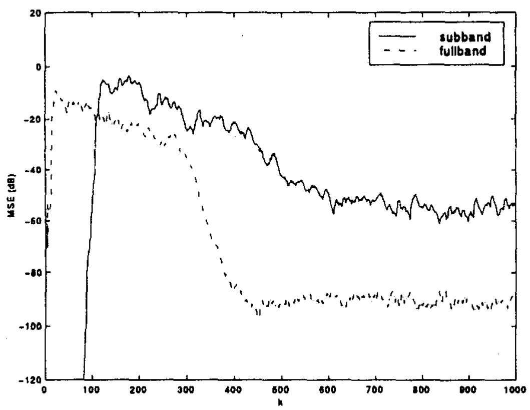

Figure 6: Simulation results with colored input.

VI. CONCLUSIONS

We have derived the adaptation algorithm based on the conventional RLS algorithm for a new subband structure with critical sampling, which requires the adaptation of only M subfilters in an M-band scheme.

The convergence behavior of the new adaptive subband structure has been compared to the fullband RLS algorithm. The computational complexity of the new subband structure has also been discussed. It is worth mentioning that the proposed algorithm is to be applied whenever a subband adaptive filter is required and also a fast convergence is necessary.

BIBLIOGRAPHY

[1] A. Gilloire and M. Vetterli, "Adaptive filtering in subbands with critical sampling: analysis, experiments, and application to acoustic echo cancellation," *IEEE Trans. Signal Processing*, pp. 1862-1875, vol. 40, no. 8, Aug. 1992.

[2] M. R. Petraglia and S. K. Mitra, "Performance analysis of adaptive filter structures based on subband decomposition," in *Proc. IEEE Int. Symp. Circ. Syst.*, pp. 60-63, Chicago, IL, May 1993.

[3] M. R. Petraglia, and R. G. Alves, "New Results on Adaptive Filtering Using Filter Banks," *Proc. IEEE Int. Symp. on Circuits and Systems*, pp. 2321-2324, Hong Kong, June 1997.

[4] G. Strang and T. Nguyen, *Wavelets and Filter Banks.* Wellesley - Cambridge Press, 1996.

[5] S. Haykin, *Adaptive Filter Theory*, 3nd ed., Prentice-Hall, Englewood Cliffs, New Jersey, 1996.

[6] P. S. R. Diniz, *Adaptive Filtering: Algorithms and Practical Implementation.* Kluwer Academic Publishers, Boston, MA, 1997.